
Evaluating Robot Policies in a World Model

Julian Quevedo^{*1} Percy Liang¹ Sherry Yang¹²³,
 Stanford University¹ New York University² Google DeepMind³
<https://world-model-eval.github.io>

Abstract

Robotics has broad applications from automating house chores to taking care of patients. However, evaluating robot control policies is challenging, as real-world testing is expensive, while handcrafted simulations often fail to accurately reflect real-world conditions, resulting in poor correlation between simulated evaluation and real-world outcomes. In this work, we investigate World-model-based Policy Evaluation (WPE). We first train an action-conditioned video generation model as a proxy to real-world environments. To enable efficient rollouts of hundreds of interactive steps while mitigating error accumulation in the world model, we propose an inference scheme which we call *Blockwise-Autoregressive* Diffusion Transformer with adjustable context and decoding horizon lengths. To ensure that the world model indeed follows action input, we propose metrics based on the agreement between the ground truth video and generated video conditioned on the same sequence of actions to evaluate the world model. We then use the world model for policy evaluation by performing Monte Carlo rollouts in the world model while employing a vision-language model (VLM) as a reward function. Interestingly, we found that WPE tends to underestimate the policy values for in-distribution actions and overestimate policy values for out-of-distribution actions. Nevertheless, WPE preserves the relative rankings of different policies. In emulating real robot executions, WPE achieves high fidelity in mimicing robot arm movements as in real videos, while emulating highly realistic object interaction remains challenging. Despite this limitation, we show that a world model can serve as a starting point for evaluating robot policies before real-world deployment.²

1 Introduction

Robots can help humans in ways that range from home robots performing chores [1, 2] to hospital robots taking care of patients [3]. One of the major road blocks in the development robots lies in evaluation — how should we ensure that these robots will work reliably without causing any physical damage when deployed in the real world? Traditionally, people have used *handcrafted* software simulators to develop and evaluate robot control policies [4, 5, 6]. However, handcrafted simulation based on our understanding of the physical world can be limited, especially when it comes to hardcoding complex dynamics with high degrees of freedom or complex interactions such as manipulating soft objects [7, 8, 9]. As a result, the sim-to-real gap has hindered progress in robotics [10, 11, 12].

With the development of generative models trained on large-scale video data [13, 14, 15], recent work has shown that video world models can visually emulate interactions with the physical real world, by conditioning on control inputs in the form of text [16, 17] or keyboard strokes [18]. This brings up an interesting question — could video world models be used to emulate robot interactions with the real world, hence being used to evaluate robot policies in the world model before real-world testing or deployment?

^{*} Correspondence to julianq@stanford.edu and sherryy@google.com.

²See videos and code at <https://world-model-eval.github.io>

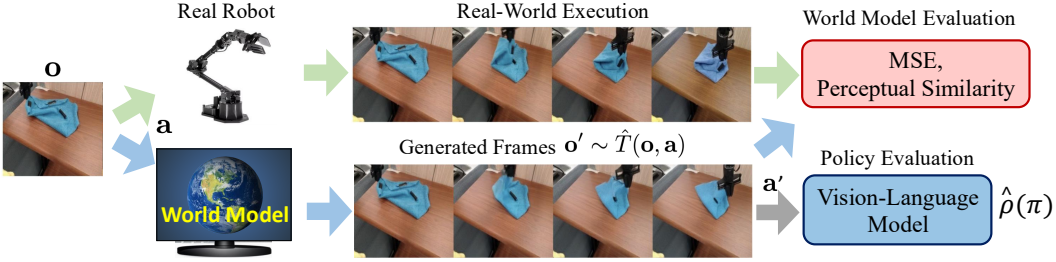


Figure 1: Overview of WPE. Generated video frames (bottom) are compared against ground-truth video frames (top) given the *same* action sequence. Semantic segmentation and tracking can evaluate the dynamics of the generative simulator, while VLMs can be used as reward models to compute policy values. Agreement between real-world videos and generated videos reflects the quality of the world model.

Learning a dynamics model from past experience and performing rollouts in the learned dynamics model has been extensively studied in model-based reinforcement learning (RL) [19, 20, 21, 22]. However, most of the existing work in model-based RL considers single-task settings, which puts itself at a disadvantage compared to model-free RL, since learning a dynamics model can be much harder than learning a policy in the single-task setting. Nevertheless, we make the important observation that

While there can be many tasks and policies, there is only one physical world in which we live that is governed by the same set of physical laws.

This makes it possible to learn a single world model that, in principle, can be used to evaluate any policies on any tasks.

Inspired by this observation, we propose World-model-based Policy Evaluation (WPE), as shown in Figure 1, by learning a *single* world model that generates videos conditioned on actions from diverse tasks and environments. Since a policy might require thousands of interactive steps to complete a task, naïvely rolling out a policy in a next-frame prediction model (similar to existing model-based RL) leads to slowdowns and error accumulations. To overcome this challenge, we propose a *Blockwise Autoregressive Transformer Diffusion* inference scheme with adjustable context and decoding lengths. With video rollouts from the world model, WPE uses a vision-language model (VLM) to determine tasks success from generated videos. We further offer practical insights on the choices of action representations, context lengths, and block-wise decoding lengths for best generation results.

Before evaluating robot policies, we first verify the dynamics and reward function of the world model by measuring their agreement both with a handcrafted software simulator [23] and with a set of real-robot videos. We then use the world model to evaluate a simulated robot policy by rolling out the policy both in the software simulator and in the world model, and compare their success rates (policy values). Our result suggests that WPE preserves the relative rankings of different policies. Interestingly, WPE underestimates in-distribution actions (actions from the policy that curated the data for training the world model) while overestimates the value for out-of-distribution actions. In emulating real-robot interactions, WPE can simulate gripper controls across different control axes highly effectively. Although simulating realistic object interactions remains challenging, we believe WPE can serve as a highly useful tool to sanity check robot policies before deploying them on real robots. Key contributions of this paper include:

- We propose to use video world model to evaluate robot policies and perform a comprehensive set of studies using software simulators and real-robot videos to understand its feasibility.
- We propose an inference scheme (Blockwise Autoregressive Transformer Diffusion) for fast inference and minimal error accumulation rollouts with hundreds of interactive steps.
- We propose evaluation metrics for the world model based on agreement between generated videos and ground-truth videos conditioned on the same sequences of actions.
- We study how action representation, context length, and generation horizon length affect the fidelity of simulation, offering practical advice for future development of generative simulators.

2 Problem Formulation

In this section, we first define relevant notations and review the formulation of offline policy evaluation (OPE). Next, we situate OPE in practical settings with partially observable environments and image-based observations, and motivate a model-based approach for tackling this practical problem.

Multi-Task POMDP. We consider a multi-task, finite-horizon, partially observable Markov Decision Process (POMDP) [24, 25], specified by $\mathcal{M} = (S, A, O, G, R, T, \mathcal{E}, H)$, which consists of a state space, action space, observation space, goal space, reward function, transition function, emission function, and horizon length. A policy π interacts with the environment for a goal starting from an initial state $g, s_0 \sim G$, producing a distribution $\pi(\cdot | s_t, g)$ over A from which an action a_t is sampled and applied to the environment at each step $t \in [0, H]$. The environment produces a scalar reward $r_t = R(s_t, g)$, and transitions to a new state $s_{t+1} \sim T(s_t, a_t)$ and emits a new observation $o_{t+1} \sim \mathcal{E}(s_{t+1})$. We consider the sparse reward setting with $R(s_H, g) \in \{0, 1\}$ and $R(s_t, g) = 0, \forall t < H$, where g is a language goal that defines the task. Data is logged from previous interactions into an offline dataset $D = \{g, s_0, o_0, a_0, \dots, s_H, o_H, r_H\}$. The value of a policy π can be defined as the total expected future reward:

$$\rho(\pi) = \mathbb{E}[R(s_H, g) | s_0, g \sim G, a_t \sim \pi(s_t, g), s_{t+1} \sim T(s_t, a_t), \forall t \in [0, H]]. \quad (1)$$

Estimating the value of $\rho(\pi)$ from previously collected data D , known as offline policy evaluation (OPE) [26], has been extensively studied [27, 28, 29, 30, 31]. However, existing work in OPE mostly focuses on simulated settings that are less practical (e.g., assumptions about full observability, access to ground truth states).

Model-Based Evaluation in a World Model. Motivated by characteristics of a real-robot system such as image based observations, high control frequencies, diverse offline data from different tasks/environments, and the lack of access to the ground truth state of the world, we propose to use the offline data to learn a *single* world model $\hat{T}(\cdot | \mathbf{o}, \mathbf{a})$, where \mathbf{o} represents a sequence of previous image observations and \mathbf{a} represents a sequence of next actions. A sequence of next observations can be sampled from the world model $\mathbf{o}' \sim \hat{T}(\mathbf{o}, \mathbf{a})$. Note that the number of frames in \mathbf{o}' and \mathbf{o} , as well as the number of actions in \mathbf{a} , can be flexibly adjusted depending on how much memory (context) is required to overcome partial observability and on the control frequency of a robot policy (how many actions it outputs at once). With this world model, we can estimate the policy value $\rho(\pi)$ with Monte-Carlo sampling using stochastic rollouts from the policy and the world model:

$$\hat{\rho}(\pi) = \mathbb{E}[\hat{R}([o_0, \dots, o_H], g) | s_0, g \sim G, \mathbf{a} \sim \pi(\mathbf{o}, g), \mathbf{o}' \sim \hat{T}(\mathbf{o}, \mathbf{a}), \mathbf{o} = \mathbf{o}'], \quad (2)$$

where \hat{R} is a learned reward function. Previously, model-free policy evaluation may be more preferable since in a single task setting, dynamics models are potentially harder to learn than policy values themselves, and doing rollouts in a dynamics model may lead to compounding errors [32]. However, we make the key observations that while there can be many tasks and many policies, there is only one physical world that is governed by the same set of physical laws. As a result, learning a world model can benefit from diverse data from different tasks and environments with different state spaces, goals, and reward functions. More importantly, a world model can be directly trained on image-based observations, which is often the perception modality of real-world robots.

3 Building a World Model Suited for Policy Evaluation

In this section, we discuss important components of a world model that is suited for policy evaluation, especially focusing on how to model the transition dynamics \hat{T} while mitigating error accumulation (Section 3.1), how to represent continuous actions (Section 3.2), and how to construct the reward model \hat{R} (Section 3.3). We finally provide implementation details of the world model in Section 3.4.

3.1 Blockwise Autoregressive Decoding for Long-Horizon Rollouts

While previous work has shown that text-conditioned video generation can simulate real-world interactions [16, 17], policy evaluation is a unique setting that requires highly precise controls (in response to robot actions), fast inference, and minimal error accumulation over time. Simulating hundreds of interactions by predicting the next observation autoregressively conditioning on each new action quickly accumulates error, as commonly found in model-based approaches [33]. On the other hand, predicting a block of observations conditioned on a block of actions may take too much time in typical video diffusion models that denoises each future frame from scratch [13].

To satisfy the requirement of both fast inference and minimal error accumulation, we propose a *blockwise autoregressive transformer diffusion* inference scheme as illustrated in Figure 2. Specifically, we divide up simulating a long-horizon rollout into blocks. Within each block, we use an autoregressive transformer to predict the noise levels of future frames within the same block conditioned on future actions similar to diffusion-forcing [34]. Moreover, we additionally introduce temporal attention

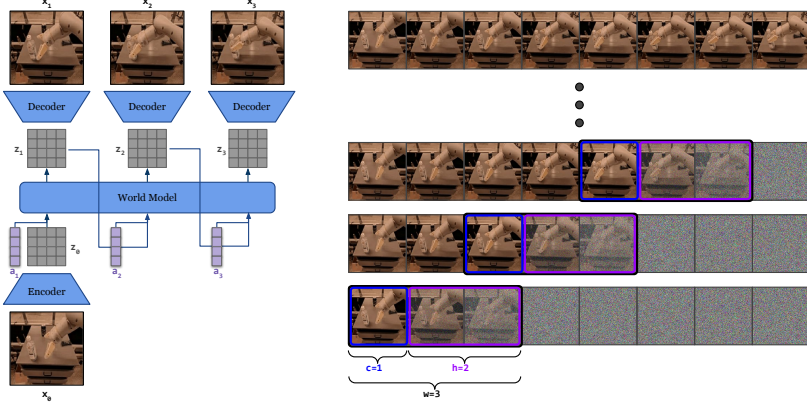


Figure 2: Inference scheme of WPE’s video generation model. WPE trains a latent video diffusion with window size w using the latent space provided by Stable Diffusion, and uses an autoregressive transformer to predict future tokens conditioned on action at each step. During inference, WPE employs a sliding window with context length c and horizon length h conditioned on h future actions. Afterwards, the sliding window is advanced forward by h frames to predict h new frames for h new actions.

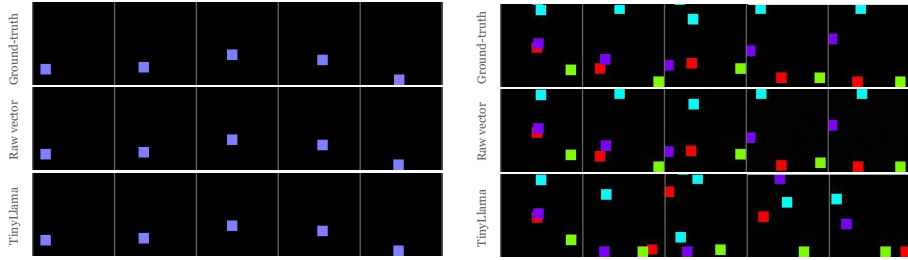


Figure 3: Gridworld Study of Action Representation. We study the most effective way to represent continuous control actions in a continuous gridworld environment where action controls the velocity of each grid. LLM embeddings (bottom row), despite using digit-wise encoding for continuous values, still loses accuracy in a system with multiple degrees of freedom in long-horizon rollouts, whereas raw continuous action vectors lead to faithful generation as the ground truth video (top row).

layers interleaved between spatial attention layers in order to provide context from previous frames to overcome any partial observability. During inference, we employ a sliding window of stride h to condition on h future actions at once to generate h future frames, then slides the window for the generation of the next block. Depending on the context length c , we can vary the amount of history that the generation conditions on by varying the size of the sliding window to overcome any partial observability.

Additional details and hyperparameters for WPE’s inference scheme can be found in Appendix A.

3.2 Action Representation

While text-to-video generation has developed a standard practice for representing text controls using language model embeddings [13, 16, 17], how to represent continuous control actions as inputs to a world model remains unclear. Naïve discretization of continuous actions loses information about precise controls, which is especially detrimental when generating hundreds of frames.

In order to understand the effect of action representation in a controlled study, we first design a simple continuous gridworld experiment as shown in Figure 3. Specifically, the action space is $A \in \mathbb{R}^{n \times 2}$ where n is the number of controllable grid blocks. Each block is controlled by a 2-dimensional velocity vector, so the actions govern the movement of the n blocks in the gridworld. One might be tempted to use LLM embeddings to represent actions, so that different action spaces can be tokenized as a text sequence. We compare the TinyLlama embedding [35], which performs digit-wise discretization and encoding, to the original raw continuous actions. We see that when the system only has a single block, LLM encoding allows perfect simulation of future frames. However, when we increase the number of blocks ($n = 3$), LLM embedding quickly loses precision in longer rollouts.

From this toy experiments, we have concluded that discretization of continuous actions and LLM embeddings are not as effective as raw continuous actions. Therefore, for all of our experiments, we use the raw continuous action vectors as inputs to WPE.

3.3 VLM as a General Reward Model

One of the major bottlenecks in video generation as a real-world simulator lies in the absence of a reward function, which software-based simulators can easily implement using heuristics such as relative locations of objects. To overcome this limitation, we parametrize $\hat{R}([o_0, \dots, o_H], g)$ using a vision-language model (VLM). Specifically, we subsample a set of generated frames from $[o_0, \dots, o_H]$, and input the frames together with the task description g to GPT-4o, and ask the VLM whether the task is successfully completed. Since VLMs are pretrained on internet-scale question-answering data similar to this type of questions, we observe high accuracy in VLMs in determining task success. Additional details on VLM as reward function, including the prompt, can be found in Appendix B.

3.4 Implementing and training the World Model

We use a Diffusion Transformer (DiT) [36] architecture similar to [37] to implement the world model. Specifically, we use the VAE from Stable Diffusion 3 [38] to encode 256×256 image frames into latent space. We employ a 16-layer transformer with 1024 hidden dimensions and 16 attention heads. To ensure that each frame does not need to be sampled from complete noise, we employ the independent per-token noise levels similar to Diffusion Forcing [34]. We train the video diffusion model on a diverse set of data sources including all of the robotic data from Open-X embodiment [39] (which contains data from 9 robots whose action spaces can be unified, such as Bridge [40] and RT-1 [41]), and data from the LIBERO software simulators [23]. We additionally rollout the OpenVLA policy [42] in the LIBERO simulator to gather more training trajectories for in-distribution policy evaluation later. We train the model using 2 A100-80GiB for 5 days. See other implementation details and hyperparameters of the world model in Appendix A.

4 Evaluating the World Model

We now evaluate the quality of the world model focusing on its dynamics (Section 4.1) and reward function (Section 4.2). We then perform ablation studies over various design decisions including scaling training data size and decoding context/horizon lengths to select the best configuration for the world model (Section 4.3). Experiment details and additional results can be found in Appendix C and D.

4.1 Evaluating Transition Dynamics \hat{T} against True Dynamics T

One advantage of a video world model is that it is highly interpretable by humans, and is hence easy to debug and evaluate visually. By conditioning the world model on the set of actions from the test split, we can visually evaluate the generated video against the ground truth video with the same action sequence.

Qualitative Evaluation. We first evaluate the world model’s ability to mimic a handcrafted simulator, LIBERO [23]. Figure 4 shows the ground truth LIBERO videos from the validation split (top) and the generated video conditioned on the same actions (bottom). For both successful (left) and unsuccessful (right), the world model is able to faithfully generate the visual dynamics. See additional qualitative results in Appendix D.

Next, we test the world model on generating similar videos as running a robot in the real world. Specifically, we take the validation split of initial images from the OpenX dataset, and predict videos conditioned on the *same* action sequences as in the original data. Figure 5 shows that the generated rollouts generally follow the real-robot rollouts across different initial observations and different robot morphologies. See additional qualitative results (including first-person view videos) in Appendix D.1.

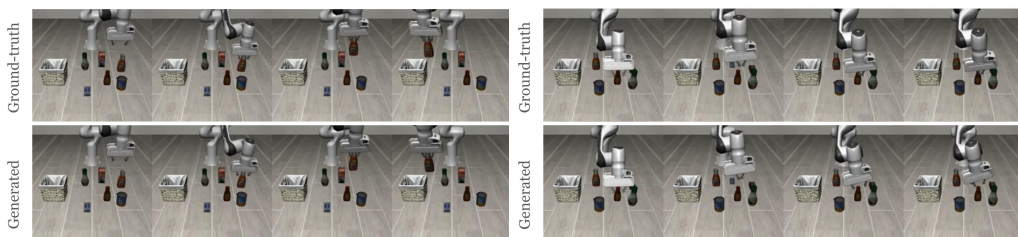


Figure 4: Qualitative evaluation of the world model on LIBERO. Within each group, Top row shows the ground truth video from a separate validation split of LIBERO. Bottom row shows the generated video from the world model. The world model faithfully generates the visual dynamics for both successful and unsuccessful rollouts.

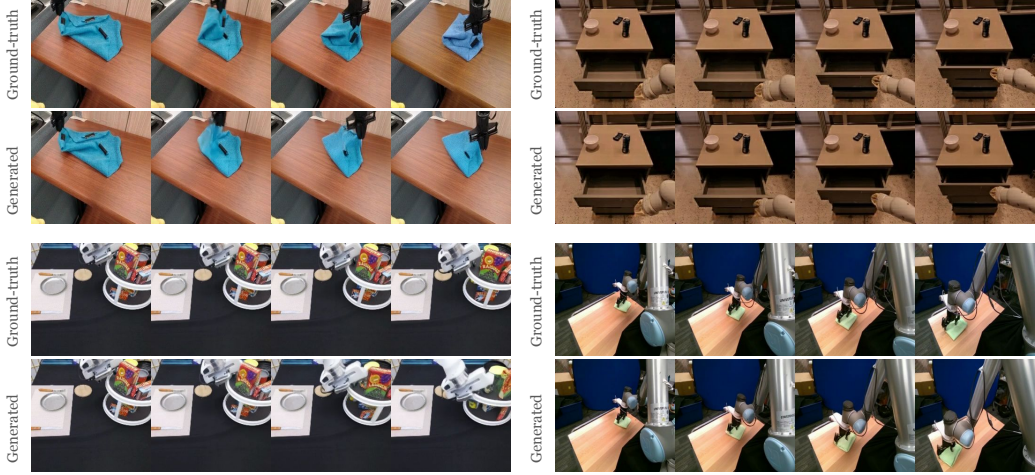


Figure 5: Qualitative evaluation of the world model on Bridge, RT-1, VIOLA, and Berkeley UR5. In each group, top row shows the ground truth video from the real robot. Bottom row shows the generated video from the world model conditioned on the same actions as the original video. The world model closely follows the true dynamics across different robot morphologies.

Quantitative Metrics. While many metrics exist for quantitatively evaluating video generation models (e.g., FVD, CLIP score, flow-based measurements), they do not capture the quality of the generated video *in response to* fine-grained action controls [43, 44]. Since this work is the first to use action-conditioned video generation to evaluate robot policies, we design metrics to evaluate the transition dynamics \hat{T} based on the agreement between the ground truth video and generated video when conditioned on the same sequence of actions.

If the world model had simulated the actions perfectly, the generated video should look *exactly the same* as the ground truth video, given that the transition dynamics is deterministic. This makes mean-squared error (MSE) between generated and ground-truth videos a natural evaluation metric. MSE has been criticized for evaluating video generation because it does not capture any uncertainty in generated videos, but we note that conditioned on the sequence of actions, there should be very little uncertainty in the generated videos. To further identify which part of a generated video do errors occur, we propose to employ a combination of semantic segmentation [45, 46] and tracking [47] to retrieve specific parts of the video (e.g., the robot arm). We can then define *semantic MSE* as the average pixel MSE of the segmented area between the ground truth video and the generated video. Formally,

$$\text{MSE}^{\text{arm}} = \mathbb{E}_{\pi, \hat{\tau}} \left[\frac{1}{H} \sum_{t=1}^H \frac{1}{|M_t^{\text{arm}}|} \sum_{(i,j) \in M_t^{\text{arm}}} (o_t(i,j) - \hat{o}_t(i,j))^2 \right] \quad (3)$$

where M_t^{arm} denotes the set of pixel indices in the segmentation mask of the robot arm at frame at time t and $o_t(i,j)$ denotes pixel values at location (i,j) of the image. Similarly, we can also compute MSE^{obj} for evaluating interactions with objects. Note that despite our focus on MSE, other pixel-wise metrics such as perceptual similarity [48] and structural similarity index (SSIM) [49] can be computed under the same setting.

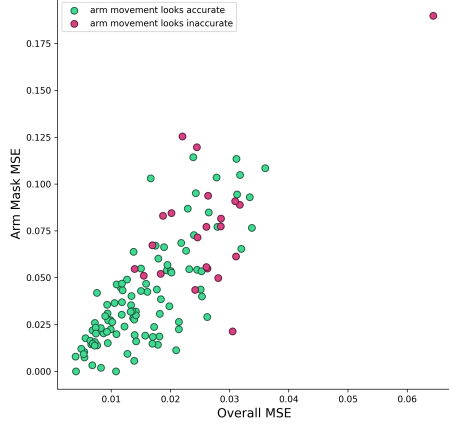


Figure 6: Relationship between MSE and human perceived success. Generated videos that are perceived as closely following ground truth (green) has lower Overall MSE (x-axis) and Arm MSE (y-axis). Occasional generated videos that are perceived as not following the ground truth (red) has higher MSE. Videos that achieve very low MSE (< 0.02) all correspond to high quality simulations according to human evaluation.

Table 1: Performance of VLM as reward (mean and standard error across 4 runs) on videos from LIBERO-Object and from RT-1 [41] using ground truth task success labels. GPT-4o achieves high true positives and true negatives. Notebaly, GPT-4o as reward has very low false positive rate, which is especially important for not over-estimating a policy value.

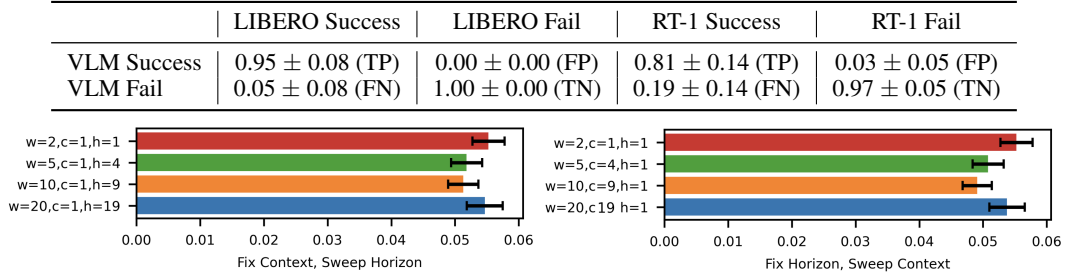


Figure 7: Ablations of context c and horizon length h (mean and standard error across 4 sets of generated videos). We found that longer context and longer horizon lengths (up to 9 frames) achieve the lowest arm MSEs, suggesting that both increasing memory and generating a longer (but not too long) sequence of video frames conditioned on a longer sequence of actions at once leads to better generation performance.

Quantitative Results. To ensure that the MSE of the arm indeed correlates with faithfulness of video generation compared to ground truth, we plot the overall MSE and the MSE of the arm of 128 generated videos for the RT-1 robot dataset in Figure 6, and label whether each rollout looks the same as the original video according to human evaluation. We found that both the overall MSE and arm MSE are low when the generated videos look similar to the original videos. Next, we compute the correlation between different video generation metrics (MSE, SSIM, and LPIPS) and human evaluation of these generated videos on whether the video looks the same as the original video. We found that MSE achieves a correlation of 0.398, SSIM achieves 0.388 while LPIPS achieves 0.415, suggesting that these metrics are similar in reflecting human perceived generation quality.

4.2 Evaluating the Reward Function \hat{R}

Evaluation Metric. To evaluate whether a vision-language model (VLM) can serve effectively as a reward function, we can take ground truth videos with ground truth labels of task success or failure, and ask a VLM if the task is successfully completed to assess the quality of the VLM by measuring its accuracy. We can further breakdown the accuracy to false positives, false negatives to better understand the types of mistakes that a VLM tends to make.

Results on LIBERO and RT-1. To determine whether VLM can serve as a reliable reward function, we take the language instruction and video as inputs to query GPT-4o of whether the task described by the language instruction was successfully completed in the video. We use whether the task is successful according to the LIBERO simulator or the RT-1 data (validation split) as the ground truth. Table 6 shows that GPT-4o achieves high true positive and true negative rate for both real and simulated videos, indicating that it is an effective evaluator of task success. Notably, GPT-4o achieves very low false positives (i.e., the rollout is a failure but the VLM thinks it is a success), which is highly useful in policy evaluation.

4.3 Ablation Studies for the World Model

In this section, we use the arm MSE metric on the Bridge data, which has been shown to be effective in evaluating a world model from Figure 6, to understand the design decisions of the world model including the choices of context and horizon lengths during decoding and scaling up training dataset size. In Figure 7, we plot the arm MSE across different context length c and horizon length h . We see that longer horizon length (9) and longer context length (9) both lead to better generation quality (lower arm MSE). However, too long of a horizon or context length (19) hurts performance. This suggests that, to a certain extent, more memory (longer context) is effective in overcoming partial observability while longer decoding horizon is effective in improving video consistency. Next, we measure MSE, LPIPS, and SSIM on generated videos from a model that is trained on less video data (Bridge-v1 [50]) and

Table 2: Dataset ablation. Larger training dataset improves all three metrics comparing generated videos and ground-truth validation videos. ↑ means higher the better.

	Subset (Bridge-v1)	Full (Bridge-v2)
MSE ↓	0.015	0.010
LPIPS ↓	0.131	0.073
SSIM ↑	0.735	0.827

Table 3: Estimated policy value $\hat{\rho}(\pi)$ for in-distribution policies (mean and standard error across 4 runs) using WPE compared to the true policy value $\rho(\pi)$ using the ground truth LIBERO simulator, where π is the OpenVLA policy from [42]. WPE achieves policy values close to the ground truth in tasks such as LIBERO-Object. WPE generally underestimates the policy value, while preserving the relative performance ordering across tasks.

Task (g)	LIBERO $\rho(\pi)$	WPE $\hat{\rho}(\pi)$
LIBERO-Spatial	0.91 ± 0.10	0.69 ± 0.06
LIBERO-Object	0.72 ± 0.16	0.56 ± 0.10
LIBERO-Goal	0.56 ± 0.22	0.28 ± 0.16
LIBERO-Long	0.47 ± 0.10	0.16 ± 0.10

Table 4: Evaluated policy value $\hat{\rho}(\pi)$ for out-of-distribution policies (mean and standard error across 4 runs) aggregated across all tasks in LIBERO. π is the OpenVLA policy from [42] with different levels of Gaussian noise. WPE overestimates the policy values across all noise levels, suggesting that evaluating out-of-distribution policies using a world model can be challenging. Nevertheless, WPE preserves the ranking of the out-of-distribution policies.

Policy Noise	LIBERO $\rho(\pi)$	WPE $\hat{\rho}(\pi)$
Noise Level 0.1	0.09 ± 0.05	0.50 ± 0.15
Noise Level 0.2	0.06 ± 0.06	0.28 ± 0.16
Noise Level 0.5	0.00 ± 0.00	0.12 ± 0.15

compare to a model that is trained on more data Bridge-v2 [40]. Table 2 shows that the model more data leads to improvements in all three metrics.

5 Evaluating Robot Policies with the World Model

After evaluating the world model, we now use the world model and WPE to evaluate policies in both simulated environments (Section 5.1) and on real-robot videos (Section 5.2). Experiment details and additional results can be found in Appendix C and D.

5.1 Emulating the LIBERO simulator

Evaluating In-Distribution Policies. We now test if WPE can achieve similar policy values as the original LIBERO simulator [23], and whether WPE can rank different policies according to their policy values [51, 52, 53]. Specifically, we evaluate the OpenVLA policy [42] (which was used to collect part of the training data for the world model and is consider an in-distribution policy) by rolling out 32 trajectories for each of the 4 LIBERO tasks. These trajectories contain hundreds of steps. In Table 3, we see that the estimated policy value using WPE is close to the true policy value in the original LIBERO simulator for LIBERO-Object. For other tasks where there exist discrepancies between $\rho(\pi)$ and $\hat{\rho}(\pi)$, $\hat{\rho}(\pi)$ always under estimates the policy value. Nevertheless, WPE preserves the ordering of the policy performance across tasks (the policy performs the best on LIBERO-Object)

Evaluating Out-of-Distribution Policies. To test whether WPE can generalize to evaluating out-of-distribution policies, we introduce Gaussian noise to the OpenVLA policy evaluated above, and report the estimated policy value (according to WPE) and the ground truth policy value (according to LIBERO) in Table 4. We see that WPE significantly overestimates the policy values, suggesting that the world model is more likely to hallucinate successful executions when actions are out-of-distribution. Nevertheless, WPE is able to preserve the rankings among the policies (the least noisy policy has the highest policy value).

5.2 Emulating A Real Robot

We now test whether WPE can emulate executions of a real robot policies. Specifically, we hard-code a robot control policy by only moving one action dimension at once (and keeping the other action dimensions as zeros). The robot is then expected to move along that one action dimension with non-zero input, corresponding to moving in different horizontal and vertical directions as well as

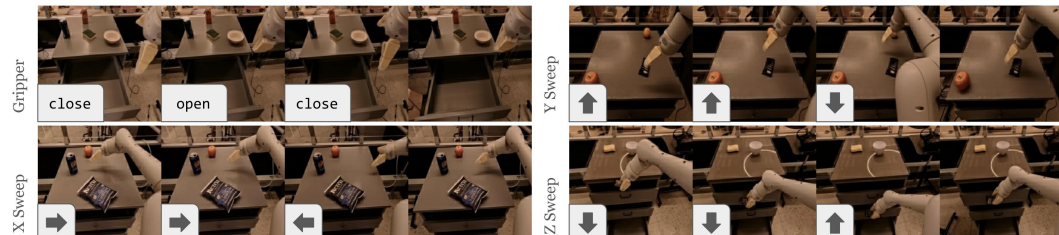


Figure 8: Results on gripper control across action dimensions. Generated videos closely follow the gripper controls such as open and close the gripper as well as moving in different directions starting from any initial observation frame.



Figure 9: Failures in simulating object interaction. While WPE can generally simulate arm movements, it sometimes fails to simulate the physics of object interactions (e.g., disappearing orange, changing object).

open and close its gripper. Figure 8 shows that the generated videos faithfully follow the gripper controls³, despite these particular sequences of gripper controls are not present in the training data.

6 Related Work

Offline Policy Evaluation. Off-policy and offline policy evaluation has long been studied in the RL literature [54, 55, 56, 57, 58, 59]. Some of these approaches are model-based, learning a dynamics model from previously collected data and rolling out the learned dynamics model for policy evaluation [19, 20, 22, 60]. Since learning a dynamics model is challenging and subjected to accumulation of error, a broader set of work has focused on model-free policy evaluation, which works by estimating the value function [61, 62, 63, 64] or policy correction [65, 66, 67]. WPE performs model-based policy evaluation, but proposes to learn a single world model on image-based observation that can be used to evaluate different policies on different tasks.

Action-Conditioned Video Generation. Previous work has shown that video generation can simulate real-world interactions [16, 17], robotic plans [68, 69], and games [37, 18, 70, 71] when conditioned on text or keyboard controls. Prior work [72] has begun to explore applying video generation to simulating complex robotic controls. We take this a step further by using video-based world models to quantitatively estimate robot policy success rates. WPE draws architectural inspirations from prior work on video generation such as Diffusion Forcing [34], Diffusion Transformers [36], and Oasis [37], but experiments with variable context and horizon lengths to support accurate long-horizon rollouts, as required in policy evaluation.

Evaluating Video Generation. Existing work on evaluating video generation models have focused on distribution-based metrics (e.g., FVD, Inception Score) for measuring diversity, text-video alignment (e.g., CLIP score, human preference score [73]) for measuring instruction following, dynamics-based metrics (e.g., optical flow [43], temporal consistency [74]), and various metrics for evaluating style and aesthetics [43]. None of the existing metrics measure precise instruction following when the instructions are continuous control actions. Some recent work has leveraged VLMs to provide feedback for video generation [44, 75], but the use of VLMs in policy evaluation, a highly useful application, has not been explored.

7 Conclusion

We have presented WPE, a framework for emulating robot interactions and evaluating robot policies in a world model using action-conditioned video generation and VLM as reward. Experimental results suggest that WPE can be highly effective in ranking different policies, and can faithfully follow gripper controls in real robot videos. Findings from WPE suggests a close connection from the large body of research in offline RL, policy evaluation, and more recently world modeling to the practical robotics applications that desperately call for safe and automatic evaluation mechanisms. WPE also opens up many interesting research questions around building physically plausible world models that can generalize to out-of-distribution actions.

Limitations. While WPE is good at emulating movements of a robot gripper, we found that emulating realistic object interactions is difficult, as shown in the failure cases in Figure 9. One potential hypothesis is that the number of frames capturing object interaction is much fewer compared to the number of frames capturing general gripper motion in the training data. Moreover, estimated policy values from WPE still have a gap from the true policy values, suggesting additional future work is required to bridge the gap between generative simulation and the real world.

³Results are best viewed as videos in the supplementary material.

Acknowledgments

We thank Xinchen Yan and Doina Precup for reviewing versions of this manuscript. We thank Moo Jin Kim for help in setting up the OpenVLA policy. We thank Boyuan Chen and Kiwhan Song for the Diffusion Forcing GitHub repository.

References

- [1] Nur Muhammad Mahi Shafiullah, Anant Rai, Haritheja Etukuru, Yiqian Liu, Ishan Misra, Soumith Chintala, and Lerrel Pinto. On bringing robots home. *arXiv preprint arXiv:2311.16098*, 2023.
- [2] Peiqi Liu, Yaswanth Orru, Jay Vakil, Chris Paxton, Nur Muhammad Mahi Shafiullah, and Lerrel Pinto. Ok-robot: What really matters in integrating open-knowledge models for robotics. *arXiv preprint arXiv:2401.12202*, 2024.
- [3] Fran Soljacic, Theresa Law, Meia Chita-Tegmark, and Matthias Scheutz. Robots in healthcare as envisioned by care professionals. *Intelligent Service Robotics*, pages 1–17, 2024.
- [4] Russ Tedrake et al. Drake: Model-based design and verification for robotics. 2019.
- [5] Emanuel Todorov, Tom Erez, and Yuval Tassa. Mujoco: A physics engine for model-based control. In *2012 IEEE/RSJ international conference on intelligent robots and systems*, pages 5026–5033. IEEE, 2012.
- [6] Tom Erez, Yuval Tassa, and Emanuel Todorov. Simulation tools for model-based robotics: Comparison of bullet, havok, mujoco, ode and physx. In *2015 IEEE international conference on robotics and automation (ICRA)*, pages 4397–4404. IEEE, 2015.
- [7] Niko Sünderhauf, Oliver Brock, Walter Scheirer, Raia Hadsell, Dieter Fox, Jürgen Leitner, Ben Upcroft, Pieter Abbeel, Wolfram Burgard, Michael Milford, et al. The limits and potentials of deep learning for robotics. *The International journal of robotics research*, 37(4-5):405–420, 2018.
- [8] Afsoon Afzal, Deborah S Katz, Claire Le Goues, and Christopher S Timperley. A study on the challenges of using robotics simulators for testing. *arXiv preprint arXiv:2004.07368*, 2020.
- [9] HeeSun Choi, Cindy Crump, Christian Duriez, Asher Elmquist, Gregory Hager, David Han, Frank Hearn, Jessica Hodgins, Abhinandan Jain, Frederick Leve, et al. On the use of simulation in robotics: Opportunities, challenges, and suggestions for moving forward. *Proceedings of the National Academy of Sciences*, 118(1):e1907856118, 2021.
- [10] Wenshuai Zhao, Jorge Peña Queralta, and Tomi Westerlund. Sim-to-real transfer in deep reinforcement learning for robotics: a survey. In *2020 IEEE symposium series on computational intelligence (SSCI)*, pages 737–744. IEEE, 2020.
- [11] Erica Salvato, Gianfranco Fenu, Eric Medvet, and Felice Andrea Pellegrino. Crossing the reality gap: A survey on sim-to-real transferability of robot controllers in reinforcement learning. *IEEE Access*, 9:153171–153187, 2021.
- [12] Gabriel Dulac-Arnold, Daniel Mankowitz, and Todd Hester. Challenges of real-world reinforcement learning. *arXiv preprint arXiv:1904.12901*, 2019.
- [13] Jonathan Ho, William Chan, Chitwan Saharia, Jay Whang, Ruiqi Gao, Alexey Gritsenko, Diederik P Kingma, Ben Poole, Mohammad Norouzi, David J Fleet, et al. Imagen video: High definition video generation with diffusion models. *arXiv preprint arXiv:2210.02303*, 2022.
- [14] Ruben Villegas, Mohammad Babaeizadeh, Pieter-Jan Kindermans, Hernan Moraldo, Han Zhang, Mohammad Taghi Saffar, Santiago Castro, Julius Kunze, and Dumitru Erhan. Phenaki: Variable length video generation from open domain textual description. *arXiv preprint arXiv:2210.02399*, 2022.
- [15] Uriel Singer, Adam Polyak, Thomas Hayes, Xi Yin, Jie An, Songyang Zhang, Qiyuan Hu, Harry Yang, Oron Ashual, Oran Gafni, et al. Make-a-video: Text-to-video generation without text-video data. *arXiv preprint arXiv:2209.14792*, 2022.

- [16] Mengjiao Yang, Yilun Du, Kamyar Ghasemipour, Jonathan Tompson, Dale Schuurmans, and Pieter Abbeel. Learning interactive real-world simulators. *arXiv preprint arXiv:2310.06114*, 2023.
- [17] Tim Brooks, Bill Peebles, Connor Holmes, Will DePue, Yufei Guo, Li Jing, David Schnurr, Joe Taylor, Troy Luhman, Eric Luhman, et al. Video generation models as world simulators. 2024. URL <https://openai.com/research/video-generation-models-as-world-simulators>, 3, 2024.
- [18] Jake Bruce, Michael D Dennis, Ashley Edwards, Jack Parker-Holder, Yuge Shi, Edward Hughes, Matthew Lai, Aditi Mavalankar, Richie Steigerwald, Chris Apps, et al. Genie: Generative interactive environments. In *Forty-first International Conference on Machine Learning*, 2024.
- [19] Raphael Fonteneau, Susan A. Murphy, Louis Wehenkel, and Damien Ernst. Batch mode reinforcement learning based on the synthesis of artificial trajectories. *Annals of Operations Research*, 208(1):383–416, 2013.
- [20] Michael R Zhang, Tom Le Paine, Ofir Nachum, Cosmin Paduraru, George Tucker, Ziyu Wang, and Mohammad Norouzi. Autoregressive dynamics models for offline policy evaluation and optimization. *arXiv preprint arXiv:2104.13877*, 2021.
- [21] Lukasz Kaiser, Mohammad Babaeizadeh, Piotr Milos, Blazej Osinski, Roy H Campbell, Konrad Czechowski, Dumitru Erhan, Chelsea Finn, Piotr Kozakowski, Sergey Levine, et al. Model-based reinforcement learning for atari. *arXiv preprint arXiv:1903.00374*, 2019.
- [22] Tianhe Yu, Garrett Thomas, Lantao Yu, Stefano Ermon, James Y Zou, Sergey Levine, Chelsea Finn, and Tengyu Ma. Mopo: Model-based offline policy optimization. *Advances in Neural Information Processing Systems*, 33:14129–14142, 2020.
- [23] Bo Liu, Yifeng Zhu, Chongkai Gao, Yihao Feng, Qiang Liu, Yuke Zhu, and Peter Stone. Libero: Benchmarking knowledge transfer for lifelong robot learning. *Advances in Neural Information Processing Systems*, 36, 2024.
- [24] Martin L Puterman. *Markov decision processes: discrete stochastic dynamic programming*. John Wiley & Sons, 2014.
- [25] Leslie Pack Kaelbling, Michael L Littman, and Anthony R Cassandra. Partially observable markov decision processes for artificial intelligence. In *International Workshop on Reasoning with Uncertainty in Robotics*, pages 146–163. Springer, 1995.
- [26] Sergey Levine, Aviral Kumar, George Tucker, and Justin Fu. Offline reinforcement learning: Tutorial, review, and perspectives on open problems. *arXiv preprint arXiv:2005.01643*, 2020.
- [27] Philip Thomas and Emma Brunskill. Data-efficient off-policy policy evaluation for reinforcement learning. In *International Conference on Machine Learning*, pages 2139–2148. PMLR, 2016.
- [28] Nan Jiang and Lihong Li. Doubly robust off-policy value evaluation for reinforcement learning. In *International conference on machine learning*, pages 652–661. PMLR, 2016.
- [29] Justin Fu, Mohammad Norouzi, Ofir Nachum, George Tucker, Ziyu Wang, Alexander Novikov, Mengjiao Yang, Michael R Zhang, Yutian Chen, Aviral Kumar, et al. Benchmarks for deep off-policy evaluation. *arXiv preprint arXiv:2103.16596*, 2021.
- [30] Mengjiao Yang, Ofir Nachum, Bo Dai, Lihong Li, and Dale Schuurmans. Off-policy evaluation via the regularized lagrangian. *Advances in Neural Information Processing Systems*, 33:6551–6561, 2020.
- [31] Philip Thomas, Georgios Theodorou, and Mohammad Ghavamzadeh. High-confidence off-policy evaluation. In *Proceedings of the AAAI Conference on Artificial Intelligence*, volume 29, 2015.
- [32] Chenjun Xiao, Yifan Wu, Chen Ma, Dale Schuurmans, and Martin Müller. Learning to combat compounding-error in model-based reinforcement learning. *arXiv preprint arXiv:1912.11206*, 2019.

- [33] Leonid Kuvayev and Richard S Sutton. Model-based reinforcement learning with an approximate, learned model. In *Proceedings of the ninth Yale workshop on adaptive and learning systems*, pages 101–105. Citeseer, 1996.
- [34] Boyuan Chen, Diego Martí Monso, Yilun Du, Max Simchowitz, Russ Tedrake, and Vincent Sitzmann. Diffusion forcing: Next-token prediction meets full-sequence diffusion. *arXiv preprint arXiv:2407.01392*, 2024.
- [35] Peiyuan Zhang, Guangtao Zeng, Tianduo Wang, and Wei Lu. Tinyllama: An open-source small language model. *arXiv preprint arXiv:2401.02385*, 2024.
- [36] William Peebles and Saining Xie. Scalable diffusion models with transformers. In *Proceedings of the IEEE/CVF International Conference on Computer Vision*, pages 4195–4205, 2023.
- [37] Decart AI, Julian Quevedo, Quinn McIntyre, Spruce Campbell, Xinlei Chen, and Robert Wachen. Oasis: A universe in a transformer. 2024.
- [38] Patrick Esser, Sumith Kulal, Andreas Blattmann, Rahim Entezari, Jonas Müller, Harry Saini, Yam Levi, Dominik Lorenz, Axel Sauer, Frederic Boesel, Dustin Podell, Tim Dockhorn, Zion English, Kyle Lacey, Alex Goodwin, Yannik Marek, and Robin Rombach. Scaling rectified flow transformers for high-resolution image synthesis, 2024.
- [39] Abby O'Neill, Abdul Rehman, Abhinav Gupta, Abhiram Maddukuri, Abhishek Gupta, Abhishek Padalkar, Abraham Lee, Acorn Pooley, Agrim Gupta, Ajay Mandlekar, et al. Open x-embodiment: Robotic learning datasets and rt-x models. *arXiv preprint arXiv:2310.08864*, 2023.
- [40] Homer Rich Walke, Kevin Black, Tony Z Zhao, Quan Vuong, Chongyi Zheng, Philippe Hansen-Estruch, Andre Wang He, Vivek Myers, Moo Jin Kim, Max Du, et al. Bridgedata v2: A dataset for robot learning at scale. In *Conference on Robot Learning*, pages 1723–1736. PMLR, 2023.
- [41] Anthony Brohan, Noah Brown, Justice Carbajal, Yevgen Chebotar, Joseph Dabis, Chelsea Finn, Keerthana Gopalakrishnan, Karol Hausman, Alex Herzog, Jasmine Hsu, et al. Rt-1: Robotics transformer for real-world control at scale. *arXiv preprint arXiv:2212.06817*, 2022.
- [42] Moo Jin Kim, Karl Pertsch, Siddharth Karamcheti, Ted Xiao, Ashwin Balakrishna, Suraj Nair, Rafael Rafailov, Ethan Foster, Grace Lam, Pannag Sanketi, et al. Openvla: An open-source vision-language-action model, 2024. URL <https://arxiv.org/abs/2406.09246>.
- [43] Ziqi Huang, Yinan He, Jiashuo Yu, Fan Zhang, Chenyang Si, Yuming Jiang, Yuanhan Zhang, Tianxing Wu, Qingyang Jin, Nattapol Chanpaisit, et al. Vbench: Comprehensive benchmark suite for video generative models. In *Proceedings of the IEEE/CVF Conference on Computer Vision and Pattern Recognition*, pages 21807–21818, 2024.
- [44] Hiroki Furuta, Heiga Zen, Dale Schuurmans, Aleksandra Faust, Yutaka Matsuo, Percy Liang, and Sherry Yang. Improving dynamic object interactions in text-to-video generation with ai feedback. *arXiv preprint arXiv:2412.02617*, 2024.
- [45] Nikhila Ravi, Valentin Gabeur, Yuan-Ting Hu, Ronghang Hu, Chaitanya Ryali, Tengyu Ma, Haitham Khedr, Roman Rädle, Chloe Rolland, Laura Gustafson, et al. Sam 2: Segment anything in images and videos. *arXiv preprint arXiv:2408.00714*, 2024.
- [46] Matt Deitke, Christopher Clark, Sangho Lee, Rohun Tripathi, Yue Yang, Jae Sung Park, Mohammadreza Salehi, Niklas Muennighoff, Kyle Lo, Luca Soldaini, et al. Molmo and pixmo: Open weights and open data for state-of-the-art multimodal models. *arXiv preprint arXiv:2409.17146*, 2024.
- [47] Cheng-Yen Yang, Hsiang-Wei Huang, Wenhao Chai, Zhongyu Jiang, and Jenq-Neng Hwang. Samurai: Adapting segment anything model for zero-shot visual tracking with motion-aware memory. *arXiv preprint arXiv:2411.11922*, 2024.
- [48] Richard Zhang, Phillip Isola, Alexei A Efros, Eli Shechtman, and Oliver Wang. The unreasonable effectiveness of deep features as a perceptual metric. In *Proceedings of the IEEE conference on computer vision and pattern recognition*, pages 586–595, 2018.

- [49] Zhou Wang, Alan C Bovik, Hamid R Sheikh, and Eero P Simoncelli. Image quality assessment: from error visibility to structural similarity. *IEEE transactions on image processing*, 13(4):600–612, 2004.
- [50] Frederik Ebert, Yanlai Yang, Karl Schmeckpeper, Bernadette Bucher, Georgios Georgakis, Kostas Daniilidis, Chelsea Finn, and Sergey Levine. Bridge data: Boosting generalization of robotic skills with cross-domain datasets. *arXiv preprint arXiv:2109.13396*, 2021.
- [51] Salvatore Corrente, Salvatore Greco, Miłosz Kadziński, and Roman Słowiński. Robust ordinal regression in preference learning and ranking. *Machine Learning*, 93:381–422, 2013.
- [52] Shengpu Tang and Jenna Wiens. Model selection for offline reinforcement learning: Practical considerations for healthcare settings. In *Machine Learning for Healthcare Conference*, pages 2–35. PMLR, 2021.
- [53] Mengjiao Yang, Bo Dai, Ofir Nachum, George Tucker, and Dale Schuurmans. Offline policy selection under uncertainty. In *International Conference on Artificial Intelligence and Statistics*, pages 4376–4396. PMLR, 2022.
- [54] Mehrdad Farajtabar, Yinlam Chow, and Mohammad Ghavamzadeh. More robust doubly robust off-policy evaluation. *arXiv preprint arXiv:1802.03493*, 2018.
- [55] Nan Jiang and Lihong Li. Doubly robust off-policy value evaluation for reinforcement learning. *arXiv preprint arXiv:1511.03722*, 2015.
- [56] Nathan Kallus and Masatoshi Uehara. Double reinforcement learning for efficient off-policy evaluation in Markov decision processes. *arXiv preprint arXiv:1908.08526*, 2019.
- [57] R. Munos, T. Stepleton, A. Harutyunyan, and M. Bellemare. Safe and efficient off-policy reinforcement learning. In *Advances in Neural Information Processing Systems*, pages 1054–1062, 2016.
- [58] Doina Precup, Richard S. Sutton, and Satinder P. Singh. Eligibility traces for off-policy policy evaluation. In *Proceedings of the 17th International Conference on Machine Learning*, pages 759–766, 2000.
- [59] P. Thomas, G. Theocharous, and M. Ghavamzadeh. High confidence off-policy evaluation. In *Proceedings of the 29th Conference on Artificial Intelligence*, 2015.
- [60] Danijar Hafner, Timothy Lillicrap, Mohammad Norouzi, and Jimmy Ba. Mastering atari with discrete world models. *arXiv preprint arXiv:2010.02193*, 2020.
- [61] Hoang Le, Cameron Voloshin, and Yisong Yue. Batch policy learning under constraints. In *International Conference on Machine Learning*, pages 3703–3712. PMLR, 2019.
- [62] Yaqi Duan and Mengdi Wang. Minimax-optimal off-policy evaluation with linear function approximation, 2020. *arXiv:2002.09516*.
- [63] Richard S Sutton, Hamid Reza Maei, Doina Precup, Shalabh Bhatnagar, David Silver, Csaba Szepesvári, and Eric Wiewiora. Fast gradient-descent methods for temporal-difference learning with linear function approximation. In *Proceedings of the 26th annual international conference on machine learning*, pages 993–1000, 2009.
- [64] Richard S Sutton, A Rupam Mahmood, and Martha White. An emphatic approach to the problem of off-policy temporal-difference learning. *Journal of Machine Learning Research*, 17(73):1–29, 2016.
- [65] Takafumi Kanamori, Shohei Hido, and Masashi Sugiyama. A least-squares approach to direct importance estimation. *The Journal of Machine Learning Research*, 10:1391–1445, 2009.
- [66] XuanLong Nguyen, Martin J Wainwright, and Michael I Jordan. Estimating divergence functionals and the likelihood ratio by convex risk minimization. *IEEE Transactions on Information Theory*, 56(11):5847–5861, 2010.

- [67] Ofir Nachum, Yinlam Chow, Bo Dai, and Lihong Li. Dualdice: Behavior-agnostic estimation of discounted stationary distribution corrections. *Advances in neural information processing systems*, 32, 2019.
- [68] Yilun Du, Sherry Yang, Bo Dai, Hanjun Dai, Ofir Nachum, Josh Tenenbaum, Dale Schuurmans, and Pieter Abbeel. Learning universal policies via text-guided video generation. *Advances in Neural Information Processing Systems*, 36, 2024.
- [69] Yilun Du, Mengjiao Yang, Pete Florence, Fei Xia, Ayzaan Wahid, Brian Ichter, Pierre Sermanet, Tianhe Yu, Pieter Abbeel, Joshua B Tenenbaum, et al. Video language planning. *arXiv preprint arXiv:2310.10625*, 2023.
- [70] Dani Valevski, Yaniv Leviathan, Moab Arar, and Shlomi Fruchter. Diffusion models are real-time game engines. *arXiv preprint arXiv:2408.14837*, 2024.
- [71] Eloi Alonso, Adam Jolley, Vincent Micheli, Anssi Kanervisto, Amos Storkey, Tim Pearce, and François Fleuret. Diffusion for world modeling: Visual details matter in atari. *arXiv preprint arXiv:2405.12399*, 2024.
- [72] NVIDIA, :, Niket Agarwal, Arslan Ali, Maciej Bala, Yogesh Balaji, Erik Barker, Tiffany Cai, Prithvijit Chattopadhyay, Yongxin Chen, Yin Cui, Yifan Ding, Daniel Dworakowski, Jiaojiao Fan, Michele Fenzi, Francesco Ferroni, Sanja Fidler, Dieter Fox, Songwei Ge, Yunhao Ge, Jinwei Gu, Siddharth Gururani, Ethan He, Jiahui Huang, Jacob Huffman, Pooya Jannaty, Jingyi Jin, Seung Wook Kim, Gergely Klár, Grace Lam, Shiyi Lan, Laura Leal-Taixe, Anqi Li, Zhaoshuo Li, Chen-Hsuan Lin, Tsung-Yi Lin, Huan Ling, Ming-Yu Liu, Xian Liu, Alice Luo, Qianli Ma, Hanzi Mao, Kaichun Mo, Arsalan Mousavian, Seungjun Nah, Sriharsha Niverty, David Page, Despoina Paschalidou, Zeeshan Patel, Lindsey Pavao, Morteza Ramezanali, Fitsum Reda, Xiaowei Ren, Vasanth Rao Naik Sabavat, Ed Schmerling, Stella Shi, Bartosz Stefaniak, Shitao Tang, Lyne Tchapmi, Przemek Tredak, Wei-Cheng Tseng, Jibin Varghese, Hao Wang, Haoxiang Wang, Heng Wang, Ting-Chun Wang, Fangyin Wei, Xinyue Wei, Jay Zhangjie Wu, Jiashu Xu, Wei Yang, Lin Yen-Chen, Xiaohui Zeng, Yu Zeng, Jing Zhang, Qinsheng Zhang, Yuxuan Zhang, Qingqing Zhao, and Artur Zolkowski. Cosmos world foundation model platform for physical ai, 2025.
- [73] Xiaoshi Wu, Yiming Hao, Keqiang Sun, Yixiong Chen, Feng Zhu, Rui Zhao, and Hongsheng Li. Human preference score v2: A solid benchmark for evaluating human preferences of text-to-image synthesis. *arXiv preprint arXiv:2306.09341*, 2023.
- [74] Weiming Ren, Huan Yang, Ge Zhang, Cong Wei, Xinrun Du, Wenhao Huang, and Wenhui Chen. Consisti2v: Enhancing visual consistency for image-to-video generation. *arXiv preprint arXiv:2402.04324*, 2024.
- [75] Achint Soni, Sreyas Venkataraman, Abhranil Chandra, Sebastian Fischmeister, Percy Liang, Bo Dai, and Sherry Yang. Videoagent: Self-improving video generation. *arXiv preprint arXiv:2410.10076*, 2024.

Appendix

A Architecture and Training Details of Video Generation

We train a diffusion transformer [36] for autoregressive next-frame prediction based on a transformer diffusion architecture similar to [37]. As in DiT [36], we embed timesteps using a 256-dimensional frequency embedding, which is then projected to the model dimensionality via a sequence of MLPs and SiLU activations. For action conditioning, we project the normalized action vector from the original robot action space to the model dimensionality via a linear transformation. The diffusion model is conditioned on both the timestep and the current action by adding their embeddings elementwise and then projecting them to $6 \times$ the transformer’s hidden size, forming the scale, shift, and gate vectors for the adaLN-Zero operations for the MLP and attention blocks.

While the architecture of our world model is similar to [37], the inference scheme is very different. [37] uses autoregressive decoding to predict each frame individually, whereas we propose blockwise parallel autoregressive decoding to reduce error accumulation.

Hyperparameter	Value
Total parameters	609 M
Image Resolution	256×256
DiT Patch Size	2
Input Channels	16
Hidden Size	1024
Layers	16
Attention Heads	16
MLP Ratio	4
Optimizer	AdamW (weight decay = 0.002, $\beta_1 = 0.9$, $\beta_2 = 0.99$)
Learning rate	8e-5
Batch size	16
Action dimension	7
Training hardware	2xA100 80GB
Training steps	300k
Diffusion noise schedule	sigmoid
Sampling timesteps	10
Prediction target	v

Table 5: Hyperparameters for training WPE’s video prediction model.

B Details of VLM as Reward

B.1 Prompt for VLM as Reward

Prompt GPT-4o as Reward \hat{R}

Here is a sequence of frames from a policy rollout video. I need your help determining whether the policy is successful. Does the robot successfully complete the following task? Explain your reasoning, and then output 'Answer: Yes' or 'Answer: No'.

Task: {task_description}

Note: The Task description may have been truncated a bit.

Note: Since the video is low resolution, disregard specific object identities in the Task description when necessary. This is because the specific object may be hard to identify in the frames' low level of detail. For example, if the task is "Pick up the X and place it in the basket", then any rollout which picks up any object and places it in the basket would be considered a success.

B.2 VLM Accuracy Across Tasks Using Suboptimal Prompt

We found that prompt tuning is important to achieve high VLM accuracy in determining task success. At an earlier version of this work, we used only the first and last frame to prompt GPT-4o to determine task success. The accuracy with $R(o_0, o_H, g)$ is reported below, which is significantly lower than passing the entire video.

Table 6: Accuracy of VLM as reward across different tasks when only using the start and end frame of a video for prompting. We found that the accuracy of the VLM is significantly improved when the entire video is passed as input.

Task (g)	LIBERO Acc ^{VLM}	WPE Acc ^{VLM}
LIBERO-Spatial	0.59	0.65
LIBERO-Object	0.71	0.77
LIBERO-Goal	0.83	0.80
LIBERO-Long	0.63	0.83

C Details of Evaluation Settings and Tasks

C.1 Gridworld Evaluation

In order to explore the effects of different action representations, we trained models on a synthetic “gridworld” task. These synthetic videos contain n colored squares, each with a random initial coordinate within the frame. At each subsequent frame, a 2-dimensional velocity is sampled for each colored square, drawn from a uniform distribution over $[-64, 64]$ pixel units. The velocity is added to the respective cube’s position, resulting in a new randomized location. The action $a \in \mathbb{R}^{2n}$ is then the concatenation of the n velocity vectors.

Since the n squares are each assigned a color deterministically, the position of each 2-vector forms a one-to-one mapping with its corresponding colored square. Thus, if a sufficiently parameterized model learns a proper representation of the action space, it should be able to learn the relatively simple operation of adding the velocity vectors to the each cube’s current position, and therefore be able to predict the next frame accurately.

We train models of 34 M parameters, conditioning on either the raw action vector or a language model encoding of it. We use a window size of 5 frames and a horizon length of 1 for all models.

C.2 Additional Details of LIBERO Evaluation

We estimates the policy values for the OpenVLA policy for solving the LIBERO tasks by rolling out 32 trajectories for each of the 4 LIBERO tasks. We then use each subset of 8 rollouts as a group to compute the accuracy, and use the 4 groups to compute the error bars. For out-of-distribution evaluation, we introduce Gaussian noise to the policy with standard deviation 0.1, 0.2, 0.5 respectively to represent 3 policies with different levels of performance.

C.3 Additional Details of Real-Robot Video Evaluation

Real robot video evaluations across different morphologies are conducted on a hold out split of OpenX Embodiment dataset [39] for the world model that is trained on the training split of OpenX Embodiment. For the decoding horizon and context length ablations, we fix the horizon and ablate over context lenght or fix the context length and ablate over the horizon lengths. For the dataset ablation studies, the model was trained only on either Bridge V1 [50] or Bridge V2 [40] (with additional data added to Bridge V1). To compute the segmented MSE, we use SAM2 [45] to retrieve the masks and use Samurai [47] to track the mask across video frames. To compute the arm MSE, we track the arm both in the ground truth video and in the generated video.

D Additional Experimental Results

D.1 Additional Results on Real-Robot Videos

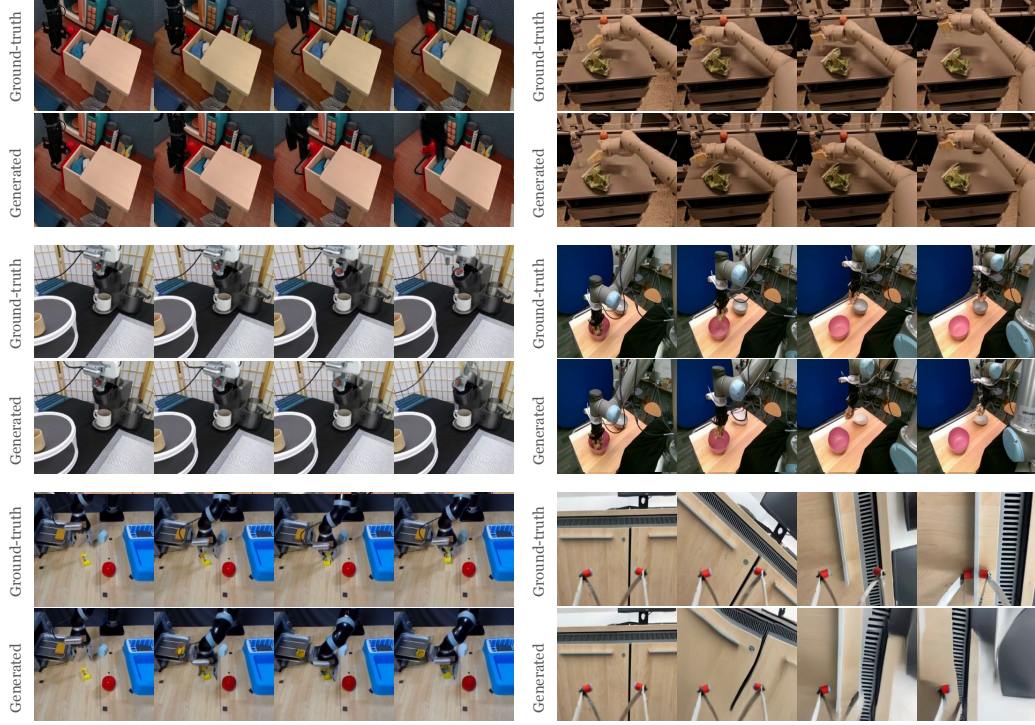


Figure 10: Additional Qualitative Evaluation of simulating actions from different robots. The world model generally generates the video that look very similar to the original video conditioned on the same actions that produced the original video in the real world.

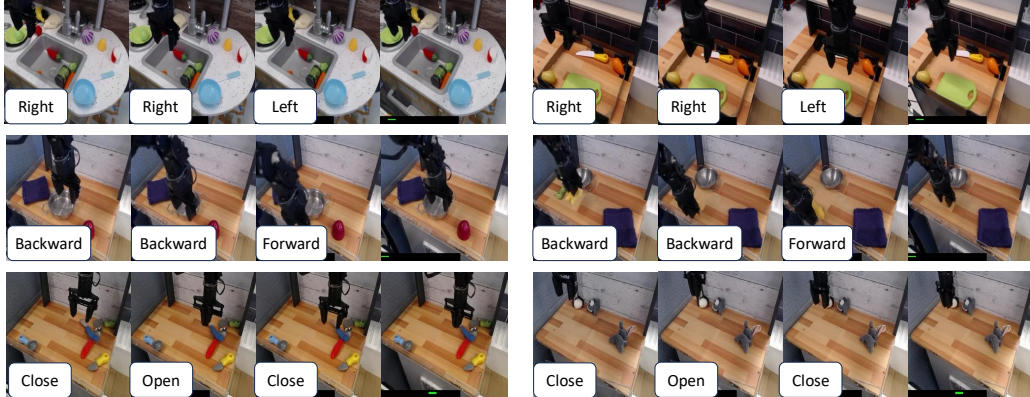


Figure 11: Additional Qualitative Evaluation of simulating different gripper controls along different action dimensions corresponding to left-right, forward-backward, and gripper open-close. The world model generally generates videos that follow the actions.

D.2 Additional Results on Emulating LIBERO Simulators

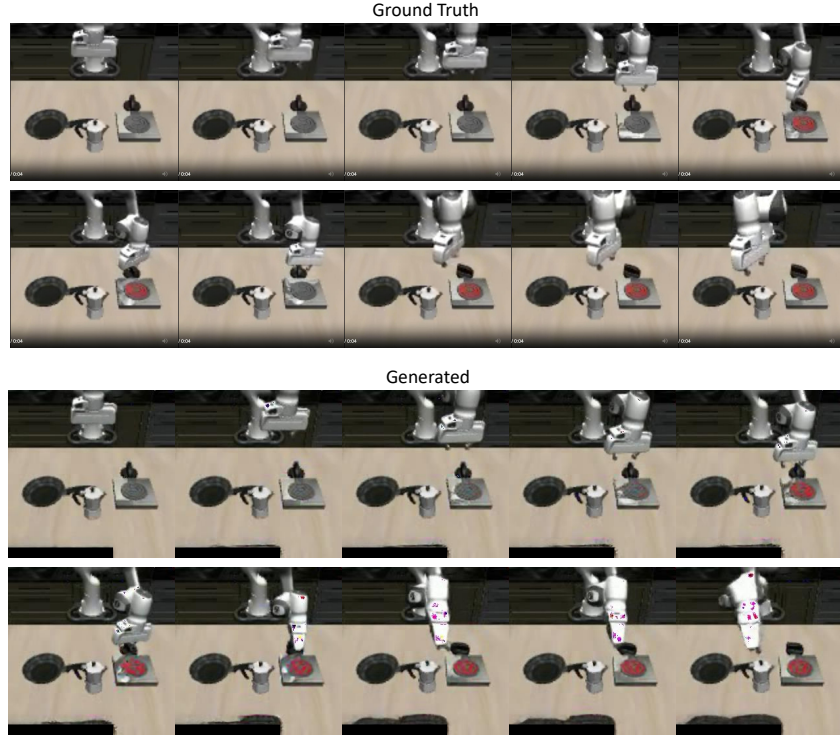


Figure 12: Additional Qualitative Evaluation of rolling out a policy in the original LIBERO simulator (top) compared to rolling out in the world model (bottom). While the world model generally reflects the movement of the gripper, object interactions lack realism as the stove turns red before the gripper turns it on (third row, right most image), and fails to turn off despite the actions have done so (bottom row).